HHS Public Access

Author manuscript

Mol Cancer Ther. Author manuscript; available in PMC 2018 May 01.

Published in final edited form as:

Mol Cancer Ther. 2017 May ; 16(5): 819–830. doi:10.1158/1535-7163.MCT-16-0444.

Dual targeting of epithelial ovarian cancer via folate receptor α and the proton-coupled folate transporter with 6-substituted pyrrolo[2,3-*d*]pyrimidine antifolates

Zhanjun Hou[*,1,2], **Leda Gattoc**[*,1], **Carrie O'Connor**[1], **Si Yang**[4], **Adrianne Wallace-Povirk**[1], **Christina George**[1], **Steve Orr**[1], **Lisa Polin**[1,2], **Kathryn White**[1], **Juiwanna Kushner**[1], **Robert T. Morris**[1,2], **Aleem Gangjee**[θ,4], and **Larry H. Matherly**[θ,1,2,3]

[1]Department of Oncology, Wayne State University School of Medicine, Detroit, MI 48201

[2]Molecular Therapeutics Program, Barbara Ann Karmanos Cancer Institute, Detroit, MI 48201

[3]Department of Pharmacology, Wayne State University School of Medicine, Detroit, MI 48201

[4]Division of Medicinal Chemistry, Graduate School of Pharmaceutical Science, Duquesne University, Pittsburgh, PA 15282

Abstract

Folate uptake in epithelial ovarian cancer (EOC) involves the reduced folate carrier (RFC) and the proton-coupled folate transporter (PCFT), both facilitative transporters, and folate receptor (FR) α. Whereas in primary EOC specimens, FRα is widely expressed and increases with tumor stage, PCFT was expressed independent of tumor stage (by real-time RT-PCR and immunohistochemistry). EOC cell line models, including cisplatin sensitive (IGROV1 and A2780) and resistant (SKOV3 and TOV112D) cells, expressed a 17-fold range of FRα and similar amounts (within ~2-fold) of PCFT. Novel 6-substituted pyrrolo[2,3-*d*]pyrimidine thienoyl antifolates **AGF94** and **AGF154** exhibited potent anti-proliferative activities toward all of the EOC cell lines, reflecting selective cellular uptake by FRα and/or PCFT over RFC. When IGROV1 cells were pretreated with **AGF94** at pH 6.8, clonogenicity was potently inhibited, confirming cell killing. FRα was knocked down in IGROV1 cells with lentiviral shRNAs. Two FRα knockdown clones (KD-4 and KD-10) showed markedly reduced binding and uptake of [^{3}H]folic acid and [^{3}H]**AGF154** by FRα, but maintained high levels of [^{3}H]**AGF154** uptake by PCFT compared to non-targeted control cells. In proliferation assays, KD-4 and KD-10 cells preserved *in vitro* inhibition by **AGF94** and **AGF154**, compared to a non-targeted control, attributable to residual FRα- and substantial PCFT-mediated uptake. KD-10 tumor xenografts in severe-compromised immune deficient mice were likewise sensitive to **AGF94**. Collectively, our results demonstrate the substantial therapeutic potential of novel 6-substituted pyrrolo[2,3-*d*]pyrimidine antifolates with

To whom correspondence should be addressed: L.H. Matherly, Molecular Therapeutics Program, Barbara Ann Karmanos Cancer Institute, 110 E. Warren Ave, Detroit, MI 48201. Tel.: 313-578-4280; Fax: 313-578-4287; matherly@karmanos.org. A. Gangjee, Division of Medicinal Chemistry, Graduate School of Pharmaceutical Sciences, Duquesne University, 600 Forbes Avenue, Pittsburgh, PA 15282. Tel: 412-396-6070; Fax: 412-396-5593; gangjee@duq.edu. Z. Hou, Molecular Therapeutics Program, Barbara Ann Karmanos Cancer Institute, 110 E. Warren Ave, Detroit, MI 48201. Tel.: 313-578-4372; Fax: 313-578-4287; houz@karmanos.org.

*θThese authors contributed equally to the work.

Disclosure of Potential Conflicts of Interest: No potential conflicts of interest were disclosed.

dual targeting of PCFT and FRα toward EOCs that express a range of FRα, along with PCFT, as well as cisplatin resistance.

Keywords

epithelial ovarian cancer; antifolate; proton-coupled folate transporter; folate receptor alpha; targeted therapeutics

INTRODUCTION

An estimated 22,280 new cases of ovarian cancer are expected in the US in 2016 (1). Ovarian cancer accounts for 5% of cancer deaths among women (14,240 in the US), far greater than any other gynecologic cancer (1). About 85% to 90% of ovarian cancers are classified as epithelial ovarian cancer (EOC).

Most EOC patients present at an advanced stage at the time of diagnosis, complicating or limiting therapeutic options. Initial management of EOC usually involves surgery, including "debulking" of any visible tumor, followed by chemotherapy with platinum-based drugs (i.e., cisplatin and carboplatin) (2). Several drugs have been combined with cisplatin or carboplatin in an attempt to improve survival, and large clinical trials have confirmed benefits of adding paclitaxel to first-line chemotherapy for women with advanced EOC (3). Although initial responses to chemotherapy approximate 70%, most EOC patients eventually relapse and develop chemoresistance (4). Clearly, there is an urgent need for new therapeutic strategies that will effect longer disease-free intervals and improve overall survival, especially for patients with platinum-resistant EOC who have limited treatment options.

Recent attention has shifted toward targeted therapies for EOC that increase tumor selectivity, while decreasing systemic toxicity (2, 4, 5). Of particular interest are therapies targeting folate receptor (FR) α (6). FRα is widely expressed in EOC, with highly elevated expression in a subset of EOC patients (6–8). Examples of FRα-targeted therapies tested clinically include a monoclonal antibody, Farletuzumab (9), IMGN853 (mirvetuximab soravtansine; a FRα-targeting antibody-drug conjugate) (10), cytotoxic folic acid conjugates [vintafolide (EC145), EC1456] (6, 7, 11), and ONX0801, a classical antifolate that is selectively transported into cells by FRs over RFC and inhibits *de novo* thymidylate biosynthesis (12). In 2016, the FDA granted orphan drug designation to IMGN853 for the treatment of ovarian cancer.

While FRs can mediate cellular uptake of folates, the majority of folate uptake into tissues and tumors involves facilitated carriers, the reduced folate carrier (RFC) and the proton-coupled folate transporter (PCFT) (13–15). RFC is ubiquitously expressed (14), whereas PCFT has more limited distribution in normal tissues (16). PCFT is widely expressed in several human solid tumors and exhibits an acidic pH optimum with high levels of transport activity at pHs characterizing the tumor microenvironment (16–18).

We discovered a novel 6-substituted 2-amino-4-oxo-pyrrolo[2,3-*d*]pyrimidine scaffold with a thieno side chain (i.e., **AGF94**) with a high level of selectivity for FR and PCFT over RFC

(Figure 1) (19). Most recently, we reported the synthesis and biological activities of a 2′,4′-thienoyl regioisomer of **AGF94, AGF154** (Figure 1) (20). Both **AGF94** and **AGF154** inhibited proliferation of IGROV1 and SKOV3 EOC cells *in vitro*, despite ~5-fold differences in relative levels of FRα (SKOV3<IGROV1) (20). This is likely attributable to cellular uptake by PCFT, in addition to FRα. Cytotoxicity was directly attributable to inhibition of *de novo* purine nucleotide biosynthesis at glycinamide ribonucleotide formyltransferase (GARFTase), the first folate-dependent step. These results were further tested *in vivo*, whereby **AGF94** and **AGF154** exhibited similar antitumor efficacies toward early-stage SKOV3 EOC xenografts, with modest toxicity, reflecting their tumor-selective uptake by FR and PCFT over RFC (20).

In this report, we further explore the broader therapeutic potential of PCFT-targeted agents for EOC, including antitumor activities of 6-substituted pyrrolo[2,3-*d*]pyrimidine antifolates **AGF94** and **AGF154** toward a spectrum of EOC cell line models expressing a wide range of FRα accompanied by PCFT, analogous to patterns measured in primary EOC specimens. Our results validate the notion of selective targeting EOC by PCFT and potent antitumor efficacies for these novel dual-targeted agents, at least in part independent of high levels of FRα and toward cisplatin resistant EOC.

MATERIALS AND METHODS

Reagents

AGF94 [(S)-2-((5-[3-(2-amino-4-oxo-4,7-dihydro-3H-pyrrolo[2,3-*d*]pyrimidin-6-yl)-propyl]-thiophene-2-carbonyl)-amino)-pentanedioic acid] and **AGF154** [(S)-2-((5-[3-(2-amino-4-oxo-4,7-dihydro-3H–pyrrolo[2,3-*d*]-pyrimidin-6-yl)-propyl]-thiophene-3-carbonyl)-amino)-pentane-dioic acid] were synthesized as previously described (19, 20). PMX [N-(4-[2-(2-amino-3,4-dihydro-4-oxo-7H-pyrrolo[2,3-*d*]pyrimidin-5-yl)ethyl]benzoyl)-L-glutamic acid] (Alimta) was obtained from Eli Lilly and Co. (Indianapolis, IN). PT523 (N(alpha)-(4-amino-4-deoxypteroyl)-N(delta)-hemiphthaloyl-L-ornithine) (21) was a gift of Dr. Andre Rosowsky (Boston, MA). Leucovorin [(6R,S) 5-formyl tetrahydrofolate] (LCV) was obtained from the Drug Development Branch, National Cancer Institute, Bethesda, MD. [^{3}H]Folic acid (27.2Ci/mmol) and [^{3}H]**AGF154** (12.3 Ci/mmol) were purchased from Moravek Biochemicals (Brea, CA). Other chemicals were obtained from commercial sources in the highest available purity. Cisplatin was purchased from Tocris Bioscience (Bristol, United Kingdom).

Real-time RT-PCR analysis of folate-related transcripts

Patient cDNAs were purchased from Origene (Rockville, MD), including 41 EOC specimens (16 stage I; 3 stage II; 19 stage III; and 3 stage IV) and 7 normal ovary specimens. RNAs were isolated from the EOC cell lines (below) using TRIzol reagent (Life Technologies, Carlsbad, CA). cDNAs were synthesized with random hexamers and MuLV reverse transcriptase (including RNase inhibitor) (Applied Biosystems, Waltham, MA) and were purified using a QIAquick PCR Purification Kit (QIAGEN, Valencia, CA). Quantitative real-time RT-PCR was performed using a Roche LightCycler 480 (Roche Diagnostics, Indianapolis, IN) with gene-specific primers for FRα and PCFT and FastStart

DNA Master SYBR Green I Reaction Mix (Roche Diagnostics). Primer sequences are available upon request. Transcript levels were normalized to transcript levels of glyceraldehyde-3-phosphate dehydrogenase (GAPDH) or β-actin.

Immunohistochemistry

Tissue microarray (TMA) (OV802a) and immunohistochemistry (IHC) services were purchased from US Biomax, Inc. (Rockville, MD). The array included 47 EOC specimens (22 stage I; 12 stage II; 10 stage III; and 3 stage IV) and 10 unmatched adjacent normal ovary tissues. The tissues were formalin-fixed and paraffin-embedded. The TMAs were deparaffinized, rinsed, microwaved, and incubated with polyclonal antibody to human PCFT raised in rabbits (22). PCFT antibody was purified from serum using a peptide Affi-Gel 10 affinity column (BioRad, Richmond, CA). The slides were developed with ImmPRESS anti-rabbit IgG (peroxidase) (Vector Laboratories, Burlingame, CA) and 3,3'-diaminobenzidine tetrahydrochloride, rinsed, counterstained with Hematoxylin QS (Vector Labs, Burlingame, CA), cleared and mounted with permanent mounting medium (Sigma-Aldrich, St. Louis, MO). The slides were scanned by Aperio Image Scanner (Aperio Technologies, Inc., Buffalo Grove, IL) for microarray images. The total intensity of antibody-positive staining of each tissue core was computed and plotted.

Cell lines and culture conditions

The SKOV3 EOC cell line (23) was purchased from the American Type Culture Collection (Manassas, VA). The IGROV1 (24) and A2780 (25) EOC cell lines were generous gifts from Dr. Manohar Ratnam (Karmanos Cancer Institute) and Dr. Thomas Hamilton (Fox Chase Cancer Center, Philadelphia, PA), respectively. TOV112D cells (26) were a gift from Dr. G-S. Wu (Karmanos Cancer Institute). The SKOV3 cell line was derived from a 64-year old Caucasian patient with ovarian cancer (27). IGROV1 cells originated from the tumor of a 47-year-old woman diagnosed with stage III ovarian cancer (24). The A2780 ovarian cancer cell line was established from tumor tissue from an untreated patient (28). The TOV112D cell line was initiated in October of 1992 from a patient of French-Canadian descent with early onset ovarian cancer and an unknown family history of ovarian cancer (26). The subtypes of the EOC cell lines are as follows: IGROV1, mixed; TOV112D, endometrioid; SKOV3, serous; and A2780, non-specified (29). As warranted, the EOC cell lines were verified by Genetica DNA Laboratories (Burlington, NC) by STR profiling. IGROV1, SKOV3, and A2780 cells were cultured in RPMI 1640 medium, supplemented with 10% fetal bovine serum (Sigma-Aldrich), 1% penicillin/streptomycin (Life Technologies, Grand Island, NY), and 2 mM L-glutamine at 37° C with 5% CO_2. A2780 cells were supplemented with 50 μg/ml insulin (Sigma-Aldrich). TOV112D cells were maintained in a 1:1 mixture of MCDB105 and M199 media (Sigma-Aldrich), supplemented with 10% fetal bovine serum, 1% penicillin/streptomycin, and 2 mM L-glutamine at 37° C with 5% CO_2.

The PCFT- and RFC-null R1–11 HeLa cell line (30) was a gift from Dr. I. David Goldman (Bronx, NY) and was maintained in RPMI 1640 medium, supplemented with 10% fetal bovine serum, 1% penicillin/streptomycin, and 2 mM L-glutamine at 37° C with 5% CO_2. Prior to experiments, all cell lines were grown in folate-free RPMI 1640 (Life Technologies,

Carlsbad, CA), supplemented with 10% fetal bovine serum, 1% penicillin/streptomycin, and 2 mM L-glutamine for at least two weeks.

For cell proliferation assays, the EOC cell lines were plated in 96-well culture plates (4000 cells/well; 200 μl/well) with complete folate-free RPMI 1640 including dialyzed fetal bovine serum, L-glutamine, and antibiotics, supplemented with 2 or 25 nM LCV, as appropriate. Drugs were added, with concentrations from 1 to 1000 nM for **AGF94, AGF154**, PMX, and PT523, and from 0.001 to 10 μM for cisplatin. Cells were incubated from 96 to 120 h (depending on the cell line) at 37° C in a CO_2 incubator. Cell viabilities were measured with a fluorescence-based viability assay (CellTiter-Blue®; Promega, Madison, WI) and a fluorescence plate reader (emission at 590 nm, excitation at 560 nm) for calculating the drug concentrations that inhibit growth by fifty percent (IC_{50}). To demonstrate FRα-mediated drug uptake, excess (200 nM) folic acid was added to parallel cultures. Under these conditions, cellular uptake by PCFT was unaffected (20).

For colony-forming assays, IGROV1 cells (10,000 cells) were plated into 100 mm dishes in folate-free RPMI 1640 medium (pH 7.2), supplemented with 10% dialyzed fetal bovine serum, 1% penicillin/streptomycin, 2 mM L-glutamine, with 25 nM LCV. After 24 h, the cells were treated with **AGF94** or PMX (0, 0.1, 0.5, 1, 5, 10 and 20 μM) for an additional 24 h in the above media at pH 6.8, followed by outgrowth in same media at pH 7.2 without drug. To maintain pH 6.8 and pH 7.2, the media was supplemented with 25 mM PIPES/25 mM HEPES (18) and 100 mM HEPES, respectively. After treatment, cells were rinsed with Dulbecco's phosphate-buffered saline (PBS), and complete folate-free RPMI 1640 medium (pH 7.2) with dialyzed fetal bovine serum, antibiotics, and 25 nM LCV was added. Following incubation for 12 days, the dishes were washed with PBS, 5% trichloroacetic acid (TCA), and borate buffer (10 mM, pH 8.8). The colonies were stained with 1% methylene blue (in borate buffer), the dishes were rinsed with borate buffer, and colonies were counted with a GelCount™ colony counter (Oxford Optronix, UK).

Generation of IGROV1 FRα knockdown cells

IGROV1 cells were seeded at 2×10^5 cells per well in 24 well dishes, containing standard RPMI 1640, supplemented with 10% fetal bovine serum, 1% penicillin/streptomycin, and 2 mM L-glutamine, with the addition of 4 μg/mL polybrene and 10^5 TU of MISSION® lentiviral particles (Sigma-Aldrich), containing shRNAs targeting FRα or a non-targeted control (NTC) shRNA sequence. After 24 h, fresh medium including 2 μg/ml puromycin was added. Confluent cultures were trypsinized, and passaged 3–4 times in the presence of 2 μg/ml puromycin. The cells were plated in 100 mm dishes in complete medium with 2 μg/ml puromycin at a density of 100 cells/dish to isolate single colonies. Clones were picked and expanded; RNAs were isolated from each clonal culture for determining the extent of FRα knockdown by real-time RT-PCR (see above). Two FRα knockdown clones were isolated and characterized, designated KD-4 and KD-10. We tested 5 shRNAs, of which lentiviral particle 1 (P1; TRCN#2563SK1) gave the greatest knockdown of FRα for our studies.

Gel electrophoresis and Western blotting

The EOC cell lines were cultured, as described above. The cells (~ 2×10^7) were disrupted by sonication and cell debris removed by centrifugation (1,800 rpm, 5 min). A particulate membrane fraction was prepared by centrifugation at 37,000 x g. The membrane pellet was solubilized with 1% SDS in 10 mM Tris-HCl [pH 7, containing protease inhibitors (Roche Diagnostics)]. Membrane proteins (120 μg) were electrophoresed on 4–20% Tris/glycine gels (Life Technologies) with SDS (31) and transferred to polyvinylidene difluoride membranes (Thermo Scientific, Rockford, IL) (32). To detect PCFT, human PCFT-specific polyclonal antibody raised in rabbits to a carboxyl termini peptide (22) was used, with IRDye800CW-conjugated goat anti-rabbit IgG secondary antibody (LI-COR Biosciences, Lincoln, NE). Membranes were scanned with an Odyssey® infrared imaging system (LI-COR Biosciences, Omaha, NE). Protein loading was normalized to levels of β-actin using anti-β-actin mouse antibody (Sigma-Aldrich).

FRα binding and uptake assays

Total FRα protein levels were measured for the EOC cell lines (including IGROV1 NTC cells and KD-4 and KD-10 FRα-knockdown cells) by determining [^{3}H]folic acid binding to surface FRs (20). Briefly, cells (~$2-4\times10^6$) in a 60 mm culture dish were rinsed (3x) with ice-cold PBS, then with ice-cold acetate buffer (10 mM sodium acetate, 150 mM NaCl, pH 3.5) (2x) to remove FR-bound folates, and finally with ice-cold HEPES-buffered saline (20 mM HEPES, 140 mM NaCl, 5 mM KCl, 2 mM $MgCl_2$, 5 mM glucose, pH 7.4) (HBS) (3x). Cells were incubated in HBS with [^{3}H]folic acid (50 nM) in the presence and absence of unlabeled folic acid (10 μM) for 15 min at 0°C. The dishes were rinsed (3x) with ice-cold HBS, after which the cells were solubilized with 0.5 N NaOH. The alkaline homogenates were measured for radioactivity and proteins (33). FR-bound [^{3}H]folic acid was calculated as pmol/mg protein.

For assays of FRα-mediated [^{3}H]folic acid and [^{3}H]**AGF154** uptake by IGROV1 NTC and KD-4 and KD-10 FRα knockdown cells (34), cells were seeded at ~0.8×10^6 cells/60 mm dish three days prior to experiment. For uptake assays, the cells were washed at room-temperature 3x with PBS, then washed 2x with acetate buffer (pH 3.5). The cells were washed 2x with room-temperature Hank's balanced salts solution (HBSS) (pH 7.4), then incubated in 2 ml HBSS, containing 50 nM [^{3}H]folic acid or [^{3}H]**AGF154** in the absence and presence of 10 μM non-radioactive folic acid, at 37° C for 60 min (total cell fraction). An additional condition involved treatment with 50 nM [^{3}H]folic acid or [^{3}H]**AGF154** at 37° C for 60 min, followed by washing with acetate buffer (pH 3.5) to remove [^{3}H]substrate bound to surface FRs (intracellular fraction). Surface-bound [^{3}H]folic acid or [^{3}H]**AGF154** was measured at 0° C via the FR-binding protocol described above. Cellular proteins were solubilized with 0.5 N NaOH for determinations of cell-associated radioactivity and cell proteins, as described above. Results were expressed as pmol [^{3}H]folic acid or [^{3}H]**AGF154** per mg cell protein.

PCFT transport assays

PCFT transport assays in monolayer cultures were performed as described. For the IGROV1, SKOV3, and A2780 cell lines, cells were plated at 30–40% confluence into 60 mm dishes

containing folate-free RPMI 1640 including 10% fetal bovine serum, 2 mM L-glutamine and antibiotics. After 48 h, cellular uptakes of [^{3}H]**AGF154** (at 0.5 μM) were measured over 5 min at 37° C in MES-buffered saline (20 mM MES, 140 mM NaCl, 5 mM KCl, 2 mM $MgCl_2$, and 5 mM glucose; pH 5.5). The dishes were washed 3x with ice-cold PBS. The cells were solubilized in 0.5 N NaOH and radioactive contents and protein concentrations (33) of the alkaline cell homogenates were determined. Intracellular radioactivity was calculated in units of pmol [^{3}H]**AGF154** per mg of cell protein. To confirm PCFT-mediated transport activity, 10 μM non-radioactive **AGF94** was added to the transport incubations to block PCFT uptake. For transport assays with the TOV112D EOC cell line, assays were performed in suspension incubations. Following growth in 60 mm dishes, cells were trypsinized, collected by centrifugation, and washed 3x with PBS. The cells were collected by centrifugation and the cell pellets (1×10^7 cells) were suspended in 2 ml MES-buffered saline in the presence or absence of non-radioactive 10 μM **AGF94** for assays of [^{3}H]**AGF154** (0.5 μM) uptake over 5 min at 37°C, in a shaking water bath (35). Processing and calculation of transport samples were as described above.

In vivo antitumor efficacy of AGF94 toward IGROV1 NTC and FRα KD-10 xenografts

Cultured IGROV1 NTC and FRα KD-10 cells were implanted subcutaneously (10^7 cells/flank) into female ICR SCID mice (National Institutes of Health DCT/DTP Animal Production Program, Frederick, MD) to develop tumor xenograft models (passage 0). Mice were supplied water and food *ad libitum*. The study mice (passage 2) were maintained on a folate-deficient diet (TD.00434; Harlan Teklad, Madison, WI) commencing 14 days prior to tumor implant to ensure that serum folate levels approximated those of humans before the start of therapy. This design is analogous to those previously published (12, 19, 20).

To test drug efficacies, experimental mice were pooled, divided into groups (4 mice/group), and implanted bilaterally and subcutaneously with 30 to 60 mg tumor fragments, using a 12-gauge trocar (day 0). Chemotherapy with **AGF94** (32 mg/kg/injection; Q4dx4; 128 mg/kg total dose) began on day 3 after tumor implantation, as previously described (19), when the numbers of cells were between 10^7 and 10^8 cells (below the limit of palpation). **AGF94** was administered intravenously (0.2 ml volume). Tumors were measured with a caliper two-to-three times weekly. Mice were sacrificed (in healthy asymptomatic condition) when individual tumor burdens reached 1500 mg. Methods for protocol design, drug treatments, toxicity evaluation, and data analysis were described previously (19, 20, 36). Quantitative end points to assess antitumor activity include: (i) T/C, corresponding to tumor masses for the treatment group (T) and control group (C) tumors on a particular day (day 31 for NTC and day 24 for KD-10) when the control tumor reached 500 mg; (ii) T−C (tumor growth delay), corresponding to the median time (days) required for the treatment group (T) and control group (C) tumors to reach a predetermined size (i.e., 500 mg); and (iii) log cell kill (LCK) which equals (T-C)/3.32 x Td, where (T-C) is growth delay as defined above, and Td is the median tumor volume doubling time of the control.

Statistical Analysis

Descriptive statistics were performed using GraphPad Prism v.6.0.

RESULTS

Expression profiles for FRα and PCFT in EOC patient specimens

To broadly explore the potential of 6-substituted pyrrolo[2,3-*d*]pyrimidine antifolates typified by **AGF94** and **AGF154** for dual-targeting EOC via FRα and PCFT, we measured FRα and PCFT transcripts by real-time RT-PCR in 41 primary EOC specimens (24 serous; 8 endometrioid; 4 mucinous; and 5 undifferentiated or unclassifiable) at different disease stages (16 stage I; 3 stage II; 19 stage III; and 3 stage IV) and in 7 “unmatched” normal ovaries (from different patients). As previously reported (37), FRα transcripts were increased (median 47-fold; $p<0.05$) in EOC specimens compared to normal ovaries. FRα levels increased with stage of disease, with a ~6-fold increase (based on median values) from stage I to stage III ($p=0.0001$) (Figure 2A). FRα transcript levels in the EOC specimens spanned a ~3000-fold range. Findings of increased FRα expression accompanying more advanced stages of ovarian cancer were previously described (8, 37).

In contrast to results with FRα, there was no significant difference in median PCFT transcript levels between normal and EOC specimens and there were no significant changes in median PCFT levels with EOC stage (Figure 2B). The range of PCFT transcripts (~80-fold) was attenuated compared to FRα. PCFT protein expression patterns in EOC specimens were established by IHC of a TMA, from a separate cohort of 10 normal and 47 EOC specimens (22 stage I; 12 stage II; 10 stage III; 3 stage IV) (Figure 2C). PCFT proteins were generally high and spanned a ~44-fold range. Representative IHC results for PCFT in primary EOC specimens are shown in Figure 2D.

Histopathological and clinical information for the primary normal and EOC specimens in Figure 2A–D are included in Table S1 and Table S2 (Supplemental Data), respectively.

FRα and PCFT expression and activity in EOC cell lines

We extended our expression analysis of FRα and PCFT to EOC cell lines, including IGROV1, SKOV3, A2780, and TOV112D. Among the EOC sublines, IGROV1 cells showed the highest levels of FRα transcripts, followed by SKOV3 and A2780 (~39% and 9%, respectively, of IGROV1 levels) (Figure 3A). FRα transcripts in the TOV112D cell line were less than 0.1% of that measured in IGROV1 cells.

Real-time RT-PCR results for FRα in IGROV1, SKOV3, and A2780 cells were corroborated by results of [^{3}H]folic acid cell surface binding assays in the presence and absence of excess (10 μM) non-radioactive folic acid, a functional measure for FRα, although for the TOV112D cells, relative levels of specific [^{3}H]folic acid binding were somewhat increased compared to FRα transcripts (Figure 3B). Mean values of 8.4, 1.9, and 0.8 pmol/mg of FRα-bound [^{3}H]folic acid were measured for IGROV1, SKOV3 and A2780 cells, respectively, with lower levels of specific [^{3}H]folic acid binding (~0.5 pmol/mg) recorded in the TOV112D cells (Figure 3B). The inexact correlation between FRα gene expression and [^{3}H]folic acid binding among these cell lines likely reflects a posttranscriptional regulation of FRα (38, 39).

PCFT transcripts and proteins were also measured for the EOC sublines (Figure 3C and 3E, respectively). PCFT was highly expressed and there were only modest differences in these parameters for IGROV1, SKOV3, and A2780 cells, although PCFT protein was somewhat decreased in the TOV112D cells. PCFT transport activity was also measured (with 0.5 μM [^{3}H]**AGF154** over 5 min at 37° C) at pH 5.5 (the PCFT pH optimum). In these experiments, excess (10 μM) non-radioactive **AGF94** was added to parallel incubations as a transport competitor to demonstrate PCFT-transport specificity. Overall, uptake of [^{3}H]**AGF154** above this background level was within a ~2-fold range among the various EOC cell lines (Figure 3D). While transport generally paralleled levels of PCFT proteins (Figure 3E), the relationship was inexact as previously reported (17, 35).

Collectively, these results establish that the EOC cell line models accurately recapitulate the findings from the primary EOC specimens in that they express a broad range of FRα with relatively constant levels of PCFT.

Anti-proliferative activities of AGF94 and AGF154 toward EOC cell lines

We systematically assessed the anti-proliferative activities of the 2',4' and 2',5' thienoyl pyrrolo[2,3-*d*]pyrimidine compounds **AGF94** and **AGF154** (Figure 1) toward the EOC sublines. Results were compared to those for PMX, among the best PCFT substrates (13, 15) which is also transported into cells by RFC and FRα, and to cisplatin.

Cells were treated with the drugs (in the presence of 2 nM LCV) for 4–5 days and proliferation was assayed with a fluorescence-based assay for calculating IC_{50} values, corresponding to concentrations that inhibit growth by 50%. Under these conditions, the pH of the tissue culture medium decreases to ~pH 6.7–6.8 (40). Parallel incubations were performed with excess (200 nM) folic acid which competitively blocks FRα uptake without an impact on PCFT transport (20). **AGF94** and **AGF154** potently inhibited growth of all the EOC sublines, with IC_{50} values ranging from 0.39–110 nM (Table 1). The most potent inhibitions were toward EOC cell lines that express the highest FRα (IGROV1, SKOV3, A2780), with reduced inhibitions toward TOV112D cells. The relative impact of 200 nM folic acid in reducing drug effects was directly proportional to the level of FRα, ranging from 234–535-fold increased IC_{50}s for IGROV1 cells, to ~30–60-fold increased IC_{50}s for A2780 cells and ~2–4-fold increased IC_{50}s for the TOV112D subline. Thus, the net result of blocking FRα with folic acid was to attenuate the differences in drug sensitivity while preserving substantial (and similar) *in vitro* efficacies of **AGF94** and **AGF154** *independent* of differences in FRα levels (Table 1). **AGF94** was ~2–5-fold more potent than **AGF154** toward all the EOC sublines.

PMX showed similar potencies toward the EOC cell lines that were independent of FRα status and were minimally impacted by 200 nM folic acid (~1.5–3-fold) (Table 1). This likely reflects the modest substrate activity of PMX for FRα (20) and its high level of transport by both PCFT and RFC (13–15). Of particular interest were results that **AGF94** and **AGF154** inhibited proliferation of EOC cells with differences in cisplatin sensitivities (Table 1). Thus, IGROV1 (24) and A2780 (41) are generally considered cisplatin sensitive, whereas SKOV3 (41) and TOV112D (42) are cisplatin resistant.

We determined the impact of increased extracellular reduced folates on the anti-proliferative activities of **AGF94** compared to PMX toward IGROV1 EOC cells (Figure 4). The results showed that for IGROV1 cells at 25 nM LCV **AGF94** still significantly inhibited cell proliferation, although the IC_{50} was increased ~10-fold compared to that at 2 nM LCV (IC_{50}s of 4.14 +/− 0.94 nM at 25 nM LCV and 0.39 +/− 0.06 nM at 2 nM LCV; mean +/− standard error; n=6). **AGF94** was more potent than PMX at both concentrations of LCV (IC_{50}s for PMX of 346 +/− 26 nM at 25 nM LCV and 57.7 +/− 3.0 nM at 2 nM LCV, respectively).

As an extension of these experiments and to assess whether drug effects are *cytotoxic* at an extracellular pH approximating the microenvironmental pH of tumors (43), IGROV1 cells were treated with 0.1–20 μM **AGF94** *for 24 h* in the presence of 25 nM LCV at pH 6.8, then washed with PBS and incubated in *drug-free* medium for 12 days at neutral pH. IGROV1 cells were treated in parallel with PMX. Colonies were stained with methylene blue and electronically counted (Figure 5). With this design, **AGF94** was potently inhibitory with an IC_{50} of 1.46 μM (± 0.06 SE; n=3). Notably, our results demonstrate potent tumor cell killing by **AGF94** over 94%. Interestingly, inhibition of colony formation by PMX was surprising modest under these conditions (IC_{50}>20 μM).

These results establish that **AGF94** and **AGF154** are potent inhibitors of EOC cell lines expressing a broad range of FRα levels, at least in part reflecting their cellular uptake by PCFT. **AGF94** was cytotoxic toward IGROV1 cells at pH 6.8, approximating the microenvironment pH of tumors.

Impact of knockdown of FRα on anti-tumor drug efficacy of AGF94 and AGF154 toward IGROV1 cells

The cell proliferation experiments summarized in Table 1 demonstrate potent *in vitro* inhibitory effects of the dual FRα/PCFT-targeted compounds **AGF94** and **AGF154** toward a collection of EOC cell lines characterized by a ~17-fold range of FRα levels, accompanied by similar levels of PCFT. To further examine the impact of substantially reduced FRα levels on antitumor efficacies of **AGF94** and **AGF154**, we used lentiviral shRNAs to knockdown FRα in IGROV1 EOC cells. We tested 5 lentiviral shRNAs for FRα knockdown by real-time RT-PCR. For the shRNA particle with the greatest FRα knockdown in “mixed” (i.e., non-clonal) IGROV1 cultures, clones were isolated and expanded. Two clonal FRα knockdown cell lines, KD-4 and KD-10, were developed, both of which showed >90% loss of FRα expression by real-time RT-PCR assay, compared to NTC cells (Figure 6A, left panel).

We measured FRα surface binding and internalization of [^{3}H]folic acid and [^{3}H]**AGF154** in KD-4 and KD-10 cells, compared to NTC cells at pH 7.4, which substantially favors FRα over PCFT uptake. For these experiments, cells were washed with acid-buffered (pH 3.5) saline, neutralized, then incubated with 50 nM [^{3}H]folic acid or [^{3}H]**AGF154** at neutral pH (pH 7.4) (i) at 4°C to measure *surface* FRα-bound [^{3}H]substrate. Cells were also incubated at 37°C for 1 h, after which (ii) *total* cell-associated [^{3}H]substrate (includes sum of both [^{3}H]folic acid or [^{3}H]**AGF154** bound to surface FRα *and* internalized [^{3}H]folic acid or

[^{3}H]**AGF154**) and (iii) *internalized* [^{3}H]substrate were quantified (20, 34). For all treatments, parallel incubations were performed with 10 μM non-radioactive folic acid which competes with FR-mediated binding and uptake so as to identify the non-specific (non-FRα-mediated) radiolabeled fraction. As shown in Figure 6B, specific (total minus 10 μM folic acid-treated) [^{3}H]folic acid and [^{3}H]**AGF154** levels were substantially reduced in the total cell [25% and 31% (KD-4), and 26% and 28% (KD-10), respectively, of the NTC level], surface-bound [30% and 34% (KD-4), and 31% and 31% (KD-10), respectively, of the NTC level], and internalized [59% and 68% (KD-4), and 49% and 61% (KD-10), respectively, of the NTC level] fractions, compared to NTC cells.

We also measured PCFT transcripts and proteins in KD-4 and KD-10 cells relative to NTC IGROV1 cells. Although there was a modest decrease in these parameters (~28% and ~40%, respectively, compared to NTC cells) (Figure 6A, right panel, and 6D, respectively), this was accompanied by robust PCFT-mediated transport of [^{3}H]**AGF154** over 5 min at pH 5.5 that was proportional to levels of PCFT proteins (Figure 6C).

To assess the impact of FRα knockdown on antifolate *in vitro* efficacies toward IGROV1 EOC cells, we measured inhibition of cell proliferation by **AGF94** and **AGF154** during continuous drug exposures of KD-4 and KD-10 cells, compared to NTC cells. Additional treatments include PMX, a substrate for all three folate transport systems, as described above, and PT523 (21), a selective RFC substrate with limited uptake by FRα or PCFT (44). **AGF94** and **AGF154** inhibited KD-4 and KD-10 cells in spite of the dramatic losses of FRα, with increased IC_{50}s compared to NTC cells (~30- and ~15-fold, respectively), well below those measured for PMX but higher than those for PT523 (Table 1). These results are consistent with the measured uptakes depicted in Figures 6B and 6C. Neither PMX nor PT523 inhibitory effects were impacted by knockdown of FRα. The effect of 200 nM folic acid on **AGF94** and **AGF154** activity was generally proportional to levels of FRα. For NTC and the knockdown cells, *in vitro* drug efficacies were essentially identical in the presence of 200 nM folic acid.

Studies were extended *in vivo* for KD-10 and NTC IGROV1 tumor xenografts in SCID mice treated with **AGF94** (32 mg/kg; IV injection; Q4dx4; 128 mg/kg total dose). The study mice (passage 2) were maintained on a folate-deficient diet (TD.00434; Harlan Teklad, Madison, WI) commencing 14 days prior to tumor implant to ensure that serum folate levels approximated those of humans before the start of therapy. Under these conditions, median folate by microbiological assay is 49 nM with a range of values from 6–107 nM (n=9); there were insignificant changes in serum folate levels during the duration of drug treatment. By this analysis, the *in vivo* efficacy toward KD-10 cells, as reflected in T/C (6%), T-C (13 days) and LCK (1.5 logs or 94.5% of cells killed), was sustained and was similar to that of NTC cells (T/C=29%; T-C=15.5 days; and LCK=1.0 or 90% of cells killed) (Table 2). Thus, substantial *in vivo* antitumor efficacy is maintained in spite of dramatically reduced levels of FRα.

Collectively, these results establish that the 6-substituted pyrrolo[2,3-*d*]pyrimidine thienoyl antifolates **AGF94** and **AGF154** are potently active toward EOC cells, reflecting their extraordinary substrate activities for FRα, combined with their PCFT-targeted effects.

DISCUSSION

The antifolates, including MTX, PMX, PDX and RTX, remain an important class of drugs for treating numerous cancers (13, 45, 46). The role of RFC transport in MTX antitumor activity has been extensively documented (14, 46–48). In non–small cell lung cancer and malignant pleural mesothelioma, expression of RFC was also associated with clinical responses to treatment with PMX (49, 50), although in another study of malignant pleural mesothelioma an important role for PCFT in PMX clinical efficacy was strongly implied (51). Transport of cytotoxic antifolates by RFC into normal tissues is causal to toxicity since RFC is expressed in normal tissues as well as tumors (14). For compounds such as MTX for which RFC is a major mode of drug uptake, loss of transport due to low expression or loss-of-function mutations involving RFC is frequently encountered (14, 46–48, 51). Reflecting this, interest has focused on identifying a new generation of cytotoxic folate analogs without RFC transport, accompanying selective cellular uptake by tumor-selective mechanisms, including FRα and PCFT (13, 16, 18–20, 35, 40, 44, 52–54). As envisaged, this would decrease toxicity while circumventing transport resistance. Further, an additional benefit would result should these agents inhibit alternative cellular targets from traditional antifolates (i.e., neither dihydrofolate reductase nor thymidylate synthase).

We discovered a new generation of folate-based cytotoxic agents with tumor-targeting capabilities resulting from their selective uptake by tumors (19, 20). Our lead compounds, **AGF94** and **AGF154**, incorporate a 6-substituted 2-amino-4-oxo-pyrrolo[2,3-*d*]-pyrimidine scaffold with a thieno side chain, and are excellent substrates for *both* FRs and PCFT but are poor substrates for the ubiquitously expressed RFC. In this study, we established that these novel FRα and PCFT dual-targeted agents potently inhibit proliferation of EOC cell lines expressing substantial PCFT, accompanying a wide range of FRα levels, analogous to patterns seen in primary EOC specimens. This was further demonstrated with IGROV1 FRα knockdown cells for which there was a sustained inhibition of cell proliferation by both **AGF94** and **AGF154** *in vitro*, and anti-tumor efficacy by **AGF94** *in vivo*, independent of FRα and attributable to PCFT. As shown with IGROV1 cells, **AGF94** was uniquely cytotoxic following drug treatments in the presence of physiologic concentrations of reduced folate at an acidic pH approximating that reported for tumors (43) and which favors its membrane transport by PCFT (16, 55). In contrast, PMX was modestly cytotoxic under these conditions.

These dual FRα- and PCFT-targeted agents offer significant advantages over current iterations of solely FRα-targeted agents in various stages of clinical development for EOC (6, 7, 9–12) which would be expected to be less efficacious toward EOCs expressing modest levels of FRα. While **AGF94** and **AGF154** inhibit proliferation and effect cytotoxicity even toward EOC cells characterized by very low FRα levels (but still mediated in part by FRα), activity was clearly enhanced by the presence of PCFT. As **AGF94** and **AGF154** are both GARFTase inhibitors in the *de novo* purine biosynthetic pathway, they deplete purines (19, 20) to limit ATP and GTP for DNA synthesis and repair, and for cellular energetics. Further, GARFTase inhibitors kill tumors independent of p53 status (56) and show tumor selectivity resulting from impaired adenine salvage, reflecting 5’-deoxy-5’-methyl thioadenosine phosphorylase deletions in many tumors (57). Another advantage of targeting purine

biosynthesis was suggested by findings of enhanced selectivity of 6-mercaptopurine and 6-thioguanine toward mutant BRCA ovarian cancers, even after the cells had acquired resistance to a PARP inhibitor or cisplatin (58). Of the EOC cell lines in this report, only IGROV1 shows mutant BRCA (as a heterogeneous 2080delA BRCA1 mutation) (59, 60). While SKOV3 and TOV112D cells are both resistant to cisplatin, they were sensitive to **AGF94**, albeit to different extents. The differential sensitivities of SKOV3 and TOV112D cells to **AGF94** are entirely consistent with differences in levels of FRα between these cell lines and to a lesser degree PCFT. Although other mechanisms could conceivably contribute to differences in **AGF94** sensitivities between these EOC cell lines [e.g., increased levels of Bcl-2 protein in TOV112D cells (61)], given their nearly identical sensitivities to both cisplatin and pemetrexed, these seem unlikely. Clearly, the ability of **AGF94** (and **AGF154**) to circumvent cisplatin resistance implies their potential for clinical implementation for EOC. Indeed, this novel series of analogs seems to offer a unique niche for targeted therapy of EOC that should be further explored.

Supplementary Material

Refer to Web version on PubMed Central for supplementary material.

Acknowledgments

This study was supported by grants from the National Cancer Institute, National Institutes of Health [R01 CA53535 (L.H. Matherly, Z. Hou), R01 CA152316 (L.H. Matherly, A. Gangjee), R01 CA166711 (A. Gangjee, L.H. Matherly)], the Wentworth Fund for Ovarian Cancer Research (R.T. Morris), the Eunice and Milt Ring Endowed Chair for Cancer Research (L.H. Matherly), and the Duquesne University Adrian Van Kaam Chair in Scholarly Excellence (A. Gangjee).

Non-Standard Abbreviations

EOC	epithelial ovarian cancer
FR	folate receptor
GAPDH	glyceraldehyde-3-phosphate dehydrogenase
GARFTase	glycinamide ribonucleotide formyltransferase
HBS	Hepes-buffered saline
HBSS	Hank’s balanced salts solution
IC_{50}	50%. inhibitory concentration
IHC	immunohistochemistry
LCS	log cell kill
LCV	leucovorin
NTC	non-targeted control
PBS	Dulbecco’s phosphate-buffered saline

PCFT	proton-coupled folate transporter
PMX	pemetrexed
RFC	reduced folate carrier
SCID	severe-combined immunodeficient
TCA	trichloroacetic acid
TMA	tissue microarray

REFERENCES

1. American Cancer Society. Cancer Facts & Figures 2016. Atlanta: American Cancer Society; 2016.
2. Korkmaz T, Seber S, Basaran G. Review of the current role of targeted therapies as maintenance therapies in first and second line treatment of epithelial ovarian cancer; In the light of completed trials. Crit Rev Oncol Hematol. 2016; 98:180–188. [PubMed: 26603345]
3. Ozols RF, Bundy BN, Greer BE, Fowler JM, Clarke-Pearson D, Burger RA, et al. Phase III trial of carboplatin and paclitaxel compared with cisplatin and paclitaxel in patients with optimally resected stage III ovarian cancer: a Gynecologic Oncology Group study. J Clin Oncol. 2003; 21:3194–3200. [PubMed: 12860964]
4. Marchetti C, Palaia I, De Felice F, Musella A, Donfracesco C, Vertechy L, et al. Tyrosine-kinases inhibitors in recurrent platinum-resistant ovarian cancer patients. Cancer Treat Rev. 2016; 42:41–46. [PubMed: 26559739]
5. Bai H, Cao D, Yang J, Li M, Zhang Z, Shen K. Genetic and epigenetic heterogeneity of epithelial ovarian cancer and the clinical implications for molecular targeted therapy. Journal of cellular and molecular medicine. 2016
6. Vergote IB, Marth C, Coleman RL. Role of the folate receptor in ovarian cancer treatment: evidence, mechanism, and clinical implications. Cancer metastasis reviews. 2015; 34:41–52. [PubMed: 25564455]
7. Assaraf YG, Leamon CP, Reddy JA. The folate receptor as a rational therapeutic target for personalized cancer treatment. Drug Resist Updat. 2014; 17:89–95. [PubMed: 25457975]
8. Chen YL, Chang MC, Huang CY, Chiang YC, Lin HW, Chen CA, et al. Serous ovarian carcinoma patients with high alpha-folate receptor had reducing survival and cytotoxic chemo-response. Molecular oncology. 2012; 6:360–369. [PubMed: 22265591]
9. Kamen BA, Smith AK. Farletuzumab, an anti-folate receptor alpha antibody, does not block binding of folate or anti-folates to receptor nor does it alter the potency of anti-folates in vitro. Cancer Chemother Pharmacol. 2012; 70:113–120. [PubMed: 22644798]
10. Kurkjian C, LoRusso P, Sankhala KK, Birrer MJ, Kirby M, Ladd S, Hawes S, Running KL, O'Leary JJ, Moore KN. A phase I, first-in-human studyto evaluate the safety, pharmacokinetics (PK), and pharmacodynamics (PD) ofIMGN853 in patients (Pts) with epithelial ovarian cancer (EOC) and other FOLR1-positive solid tumors. J Clin Oncol. 2013; 31(15 Suppl):2573.
11. Naumann RW, Coleman RL, Burger RA, Sausville EA, Kutarska E, Ghamande SA, et al. PRECEDENT: a randomized phase II trial comparing vintafolide (EC145) and pegylated liposomal doxorubicin (PLD) in combination versus PLD alone in patients with platinum-resistant ovarian cancer. J Clin Oncol. 2013; 31:4400–4406. [PubMed: 24127448]
12. Gibbs DD, Theti DS, Wood N, Green M, Raynaud F, Valenti M, et al. BGC 945, a novel tumor-selective thymidylate synthase inhibitor targeted to alpha-folate receptor-overexpressing tumors. Cancer Res. 2005; 65:11721–11728. [PubMed: 16357184]
13. Matherly LH, Wilson MR, Hou Z. The major facilitative folate transporters solute carrier 19A1 and solute carrier 46A1: biology and role in antifolate chemotherapy of cancer. Drug metabolism and disposition: the biological fate of chemicals. 2014; 42:632–649. [PubMed: 24396145]

14. Matherly LH, Hou Z, Deng Y. Human reduced folate carrier: translation of basic biology to cancer etiology and therapy. Cancer metastasis reviews. 2007; 26:111–128. [PubMed: 17334909]
15. Zhao R, Matherly LH, Goldman ID. Membrane transporters and folate homeostasis: intestinal absorption and transport into systemic compartments and tissues. Expert reviews in molecular medicine. 2009; 11:e4. [PubMed: 19173758]
16. Desmoulin SK, Hou Z, Gangjee A, Matherly LH. The human proton-coupled folate transporter: Biology and therapeutic applications to cancer. Cancer biology & therapy. 2012; 13:1355–1373. [PubMed: 22954694]
17. Wilson MR, Hou Z, Yang S, Polin L, Kushner J, White K, et al. Targeting Nonsquamous Nonsmall Cell Lung Cancer via the Proton-Coupled Folate Transporter with 6-Substituted Pyrrolo[2,3-d]Pyrimidine Thienoyl Antifolates. Mol Pharmacol. 2016; 89:425–434. [PubMed: 26837243]
18. Kugel Desmoulin S, Wang L, Hales E, Polin L, White K, Kushner J, et al. Therapeutic targeting of a novel 6-substituted pyrrolo [2,3-d]pyrimidine thienoyl antifolate to human solid tumors based on selective uptake by the proton-coupled folate transporter. Mol Pharmacol. 2011; 80:1096–1107. [PubMed: 21940787]
19. Wang L, Kugel Desmoulin S, Cherian C, Polin L, White K, Kushner J, et al. Synthesis, biological, and antitumor activity of a highly potent 6-substituted pyrrolo[2,3-d]pyrimidine thienoyl antifolate inhibitor with proton-coupled folate transporter and folate receptor selectivity over the reduced folate carrier that inhibits beta-glycinamide ribonucleotide formyltransferase. J Med Chem. 2011; 54:7150–7164. [PubMed: 21879757]
20. Wang L, Wallace A, Raghavan S, Deis SM, Wilson MR, Yang S, et al. 6-Substituted Pyrrolo[2,3-d]pyrimidine Thienoyl Regioisomers as Targeted Antifolates for Folate Receptor alpha and the Proton-Coupled Folate Transporter in Human Tumors. J Med Chem. 2015; 58:6938–6959. [PubMed: 26317331]
21. Rosowsky A, Bader H, Wright JE, Keyomarsi K, Matherly LH. Synthesis and biological activity of N omega-hemiphthaloyl-alpha,omega- diaminoalkanoic acid analogues of aminopterin and 3',5-dichloroaminopterin. J Med Chem. 1994; 37:2167–2174. [PubMed: 8035423]
22. Hou Z, Kugel Desmoulin S, Etnyre E, Olive M, Hsiung B, Cherian C, et al. Identification and functional impact of homo-oligomers of the human proton-coupled folate transporter. J Biol Chem. 2012; 287:4982–4995. [PubMed: 22179615]
23. Morimoto H, Yonehara S, Bonavida B. Overcoming tumor necrosis factor and drug resistance of human tumor cell lines by combination treatment with anti-Fas antibody and drugs or toxins. Cancer Res. 1993; 53:2591–2596. [PubMed: 7684321]
24. Benard J, Da Silva J, De Blois MC, Boyer P, Duvillard P, Chiric E, et al. Characterization of a human ovarian adenocarcinoma line, IGROV1, in tissue culture and in nude mice. Cancer Res. 1985; 45:4970–4979. [PubMed: 3861241]
25. Johnson SW, Swiggard PA, Handel LM, Brennan JM, Godwin AK, Ozols RF, et al. Relationship between platinum-DNA adduct formation and removal and cisplatin cytotoxicity in cisplatin-sensitive and -resistant human ovarian cancer cells. Cancer Res. 1994; 54:5911–5916. [PubMed: 7954422]
26. Provencher DM, Lounis H, Champoux L, Tetrault M, Manderson EN, Wang JC, et al. Characterization of four novel epithelial ovarian cancer cell lines. In vitro cellular & developmental biology Animal. 2000; 36:357–361. [PubMed: 10949993]
27. Fogh J, Wright WC, Loveless JD. Absence of HeLa cell contamination in 169 cell lines derived from human tumors. J Natl Cancer Inst. 1977; 58:209–214. [PubMed: 833871]
28. Behrens BC, Hamilton TC, Masuda H, Grotzinger KR, Whang-Peng J, Louie KG, et al. Characterization of a cis-Diamminedichloroplatinum(II)-resistant Human Ovarian Cancer Cell Line and Its Use in Evaluation of Platinum Analogues. Cancer Res. 1987; 47:414–418. [PubMed: 3539322]
29. Beaufort CM, Helmijr JC, Piskorz AM, Hoogstraat M, Ruigrok-Ritstier K, Besselink N, et al. Ovarian cancer cell line panel (OCCP): clinical importance of in vitro morphological subtypes. PLoS One. 2014; 9:e103988. [PubMed: 25230021]

30. Zhao R, Qiu A, Tsai E, Jansen M, Akabas MH, Goldman ID. The proton-coupled folate transporter: impact on pemetrexed transport and on antifolates activities compared with the reduced folate carrier. Mol Pharmacol. 2008; 74:854–862. [PubMed: 18524888]
31. Laemmli UK. Cleavage of structural proteins during the assembly of the head of bacteriophage T4. Nature. 1970; 227:680–685. [PubMed: 5432063]
32. Matsudaira P. Sequence from picomole quantities of proteins electroblotted onto polyvinylidene difluoride membranes. J Biol Chem. 1987; 262:10035–10038. [PubMed: 3611052]
33. Lowry OH, Rosebrough NJ, Farr AL, Randall RJ. Protein measurement with the Folin phenol reagent. The Journal of biological chemistry. 1951; 193:265–275. [PubMed: 14907713]
34. Elnakat H, Gonit M, Salazar MD, Zhang J, Basrur V, Gunning W, et al. Regulation of folate receptor internalization by protein kinase C alpha. Biochemistry. 2009; 48:8249–8260. [PubMed: 19639961]
35. Desmoulin SK, Wang L, Polin L, White K, Kushner J, Stout M, et al. Functional loss of the reduced folate carrier enhances the antitumor activities of novel antifolates with selective uptake by the proton-coupled folate transporter. Mol Pharmacol. 2012; 82:591–600. [PubMed: 22740639]
36. Polin, L., Corbett, TH., Roberts, BJ., Lawson, AJ., Leopold, WR., White, K., et al. Transplantable Syngeneic Rodent Tumors: Solid Tumors in Mice Tumor Models in Cancer Research. BATeicher, BA., editor. Humana Press; 2011. p. 43-78.
37. Toffoli G, Cernigoi C, Russo A, Gallo A, Bagnoli M, Boiocchi M. Overexpression of folate binding protein in ovarian cancers. Int J Cancer. 1997; 74:193–198. [PubMed: 9133455]
38. Zheng X, Kelley K, Elnakat H, Yan W, Dorn T, Ratnam M. mRNA instability in the nucleus due to a novel open reading frame element is a major determinant of the narrow tissue specificity of folate receptor α. Mol Cell Biol. 2003; 23:2202–2212. [PubMed: 12612090]
39. Antony A, Tang YS, Khan RA, Biju MP, Xiao X, Li QJ, et al. Translational upregulation of folate receptors is mediated by homocysteine via RNA-heterogeneous nuclear ribonucleoprotein E1 interactions. J Clin Invest. 2004; 113:285–301. [PubMed: 14722620]
40. Kugel Desmoulin S, Wang Y, Wu J, Stout M, Hou Z, Fulterer A, et al. Targeting the proton-coupled folate transporter for selective delivery of 6-substituted pyrrolo[2,3-d]pyrimidine antifolate inhibitors of de novo purine biosynthesis in the chemotherapy of solid tumors. Mol Pharmacol. 2010; 78:577–587. [PubMed: 20601456]
41. Hunakova L, Gronesova P, Horvathova E, Chalupa I, Cholujova D, Duraj J, et al. Modulation of cisplatin sensitivity in human ovarian carcinoma A2780 and SKOV3 cell lines by sulforaphane. Toxicol Lett. 2014; 230:479–486. [PubMed: 25159039]
42. Zucha MA, Wu ATH, Lee W-H, Wang L-S, Lin W-W, Yuan C-C, et al. Bruton's tyrosine kinase (Btk) inhibitor ibrutinib suppresses stem-like traits in ovarian cancer. Oncotarget. 2015; 6:13255–13268. [PubMed: 26036311]
43. Webb BA, Chimenti M, Jacobson MP, Barber DL. Dysregulated pH: a perfect storm for cancer progression. Nature reviews Cancer. 2011; 11:671–677. [PubMed: 21833026]
44. Wang L, Cherian C, Desmoulin SK, Polin L, Deng Y, Wu J, et al. Synthesis and antitumor activity of a novel series of 6-substituted pyrrolo[2,3-d]pyrimidine thienoyl antifolate inhibitors of purine biosynthesis with selectivity for high affinity folate receptors and the proton-coupled folate transporter over the reduced folate carrier for cellular entry. J Med Chem. 2010; 53:1306–1318. [PubMed: 20085328]
45. Monahan, BPACJ. Philadelphia, PA: Lippincott Williams and Wilkins; 2011. Antifolates; p. 109-138.
46. Gonen N, Assaraf YG. Antifolates in cancer therapy: Structure, activity and mechanisms of drug resistance. Drug Resistance Updates. 2012; 15:183–210. [PubMed: 22921318]
47. Goldman ID, Matherly LH. The cellular pharmacology of methotrexate. Pharmacol Ther. 1985; 28:77–102. [PubMed: 2414788]
48. Zhao R, Goldman ID. Resistance to antifolates. Oncogene. 2003; 22:7431–7457. [PubMed: 14576850]
49. Alvarez-Fernandez C, Perez-Arnillas Q, Ruiz-Echeverria L, Rodriguez-Rubi D, Sanchez-Lorenzo L, Li-Torres W, et al. Reduced folate carrier (RFC) as a predictive marker for response to

pemetrexed in advanced non-small cell lung cancer (NSCLC). Invest New Drugs. 2014; 32:377–381. [PubMed: 23912258]

50. Mairinger F, Vollbrecht C, Halbwedl I, Hatz M, Stacher E, Gülly C, et al. Reduced folate carrier and folylpolyglutamate synthetase, but not thymidylate synthase predict survival in pemetrexed-treated patients suffering from malignant pleural mesothelioma. Journal of thoracic oncology : official publication of the International Association for the Study of Lung Cancer. 2013; 8:644–653.
51. Giovannetti E, Zucali PA, Assaraf YG, Funel N, Gemelli M, Stark M, Leon LG, Hou Z, Perrino M, Matherly LH, Peters GJ. Role of proton-coupled folate transporter expression in resistance of mesothelioma patients treated with pemetrexed. Proceedings AACR. 2015; 56:1086.
52. Xia W, Low PS. Folate-targeted therapies for cancer. J Med Chem. 2010; 53:6811–6824. [PubMed: 20666486]
53. Wang Y, Cherian C, Orr S, Mitchell-Ryan S, Hou Z, Raghavan S, et al. Tumor-Targeting with Novel Non-Benzoyl 6-Substituted Straight Chain Pyrrolo[2,3-d]pyrimidine Antifolates via Cellular Uptake by Folate Receptor alpha and Inhibition of de Novo Purine Nucleotide Biosynthesis. J Med Chem. 2013; 56:8684–8695. [PubMed: 24111942]
54. Wang L, Cherian C, Kugel Desmoulin S, Mitchell-Ryan S, Hou Z, Matherly LH, et al. Synthesis and biological activity of 6-substituted pyrrolo[2,3-d]pyrimidine thienoyl regioisomers as inhibitors of de novo purine biosynthesis with selectivity for cellular uptake by high affinity folate receptors and the proton-coupled folate transporter over the reduced folate carrier. J Med Chem. 2012; 55:1758–1770. [PubMed: 22243528]
55. Zhao R, Goldman ID. The molecular identity and characterization of a proton-coupled folate transporter--PCFT; biological ramifications and impact on the activity of pemetrexed. Cancer metastasis reviews. 2007; 26:129–139. [PubMed: 17340171]
56. Bronder JL, Moran RG. A defect in the p53 response pathway induced by de novo purine synthesis inhibition. J Biol Chem. 2003; 278:48861–48871. [PubMed: 14517211]
57. Hori H, Tran P, Carrera CJ, Hori Y, Rosenbach MD, Carson DA, et al. Methylthioadenosine phosphorylase cDNA transfection alters sensitivity to depletion of purine and methionine in A549 lung cancer cells. Cancer Res. 1996; 56:5653–5658. [PubMed: 8971171]
58. Issaeva N, Thomas HD, Djureinovic T, Jaspers JE, Stoimenov I, Kyle S, et al. 6-thioguanine selectively kills BRCA2-defective tumors and overcomes PARP inhibitor resistance. J Cancer Res. 2010; 70:6268–6876.
59. Samouelian V, Maugard CM, Jolicoeur M, Bertrand R, Arcand SL, Tonin PN, et al. Chemosensitivity and radiosensitivity profiles of four new human epithelial ovarian cancer cell lines exhibiting genetic alterations in BRCA2, TGFbeta-RII, KRAS2, TP53 and/or CDNK2A. Cancer chemotherapy and pharmacology. 2004; 54:497–504. [PubMed: 15258697]
60. Stordal B, Timms K, Farrelly A, Gallagher D, Busschots S, Renaud M, et al. BRCA1/2 mutation analysis in 41 ovarian cell lines reveals only one functionally deleterious BRCA1 mutation. Molecular oncology. 2013; 7:567–579. [PubMed: 23415752]
61. Wang J, Zhou JY, Zhang L, Wu GS. Involvement of MKP-1 and Bcl-2 in acquired cisplatin resistance in ovarian cancer cells. Cell Cycle. 2009; 8:3191–3198. [PubMed: 19755862]

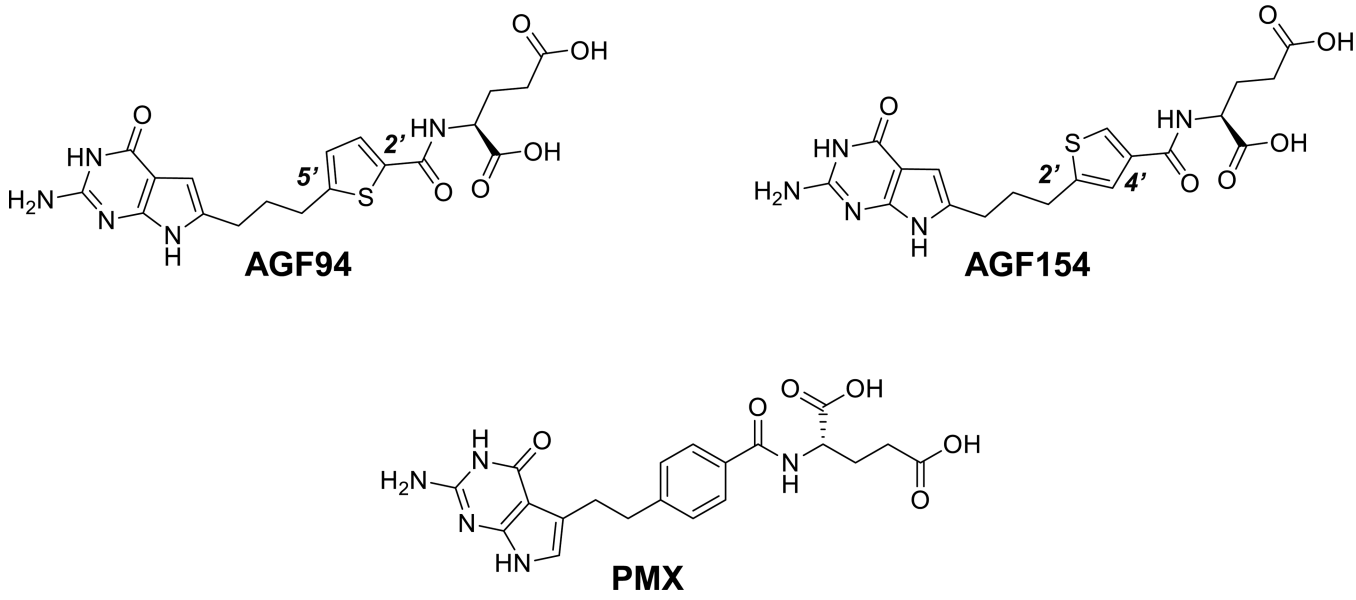

Figure 1. Structures of AGF94, AGF154, and PMX

Structures are shown for PMX, and the 6-substituted pyrrolo[2,3-*d*]pyrimidine thienoyl antifolate compounds **AGF94** and **AGF154**.

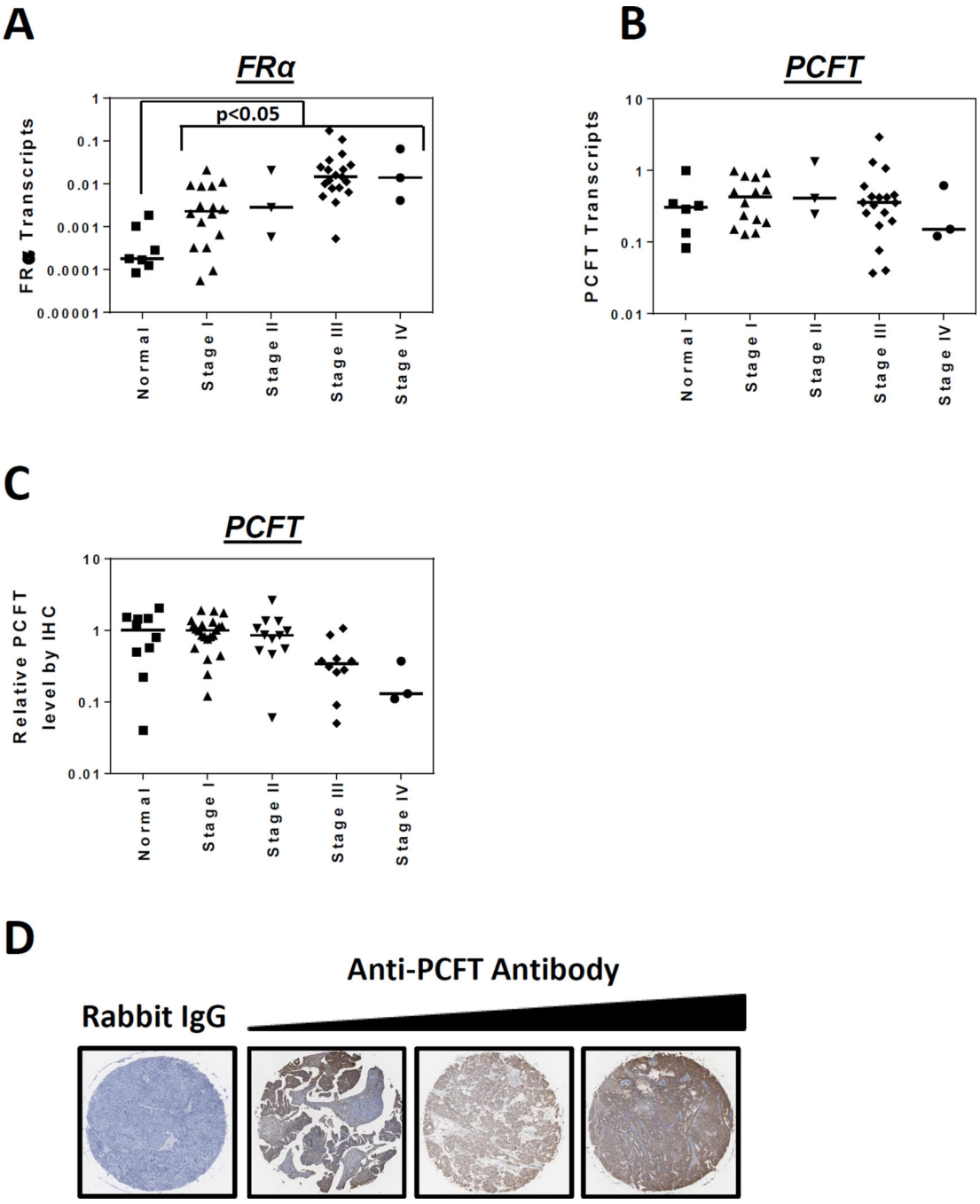

Figure 2. Expression of FRα and PCFT in primary epithelial ovarian cancer (EOC) specimens

Transcript levels for FRα (*Panel A*) and PCFT (*Panel B*) in 7 normal ovary and 41 EOC specimens from patients at different disease stages (Origene) were measured by real-time RT-PCR. FRα and PCFT transcript levels were normalized to transcript levels for β-actin. IHC staining of PCFT was performed with 47 EOC specimens and 10 normal ovary tissues from a commercial TMA (US Biomax, Inc.). The TMA was incubated with affinity-purified PCFT-specific antibody or rabbit IgG, the slides developed, counterstained and mounted, as described in Materials and Methods. The slides were scanned at 20X by an Aperio Image

Scanner (Aperio Technologies, Inc.) for microarray images. The total intensity of antibody positive staining of each tissue core was computed and plotted as a relative value with the median value for the normal ovary specimens assigned a value of 1 (*Panel C*). Statistical significance between the groups was analyzed by the Mann-Whitney t test. Median values are shown as cross bars. Representative images are shown in *Panel D* for EOC specimens incubated with IgG (specimen 35 in Table S2, Supplemental Data) and PCFT-specific antibody, with low, intermediate and high level staining (*left to right*, specimens 49, 21, and 29, respectively, in Table S2, Supplemental Data), corresponding to stages II, IIIC, I and IB, respectively.

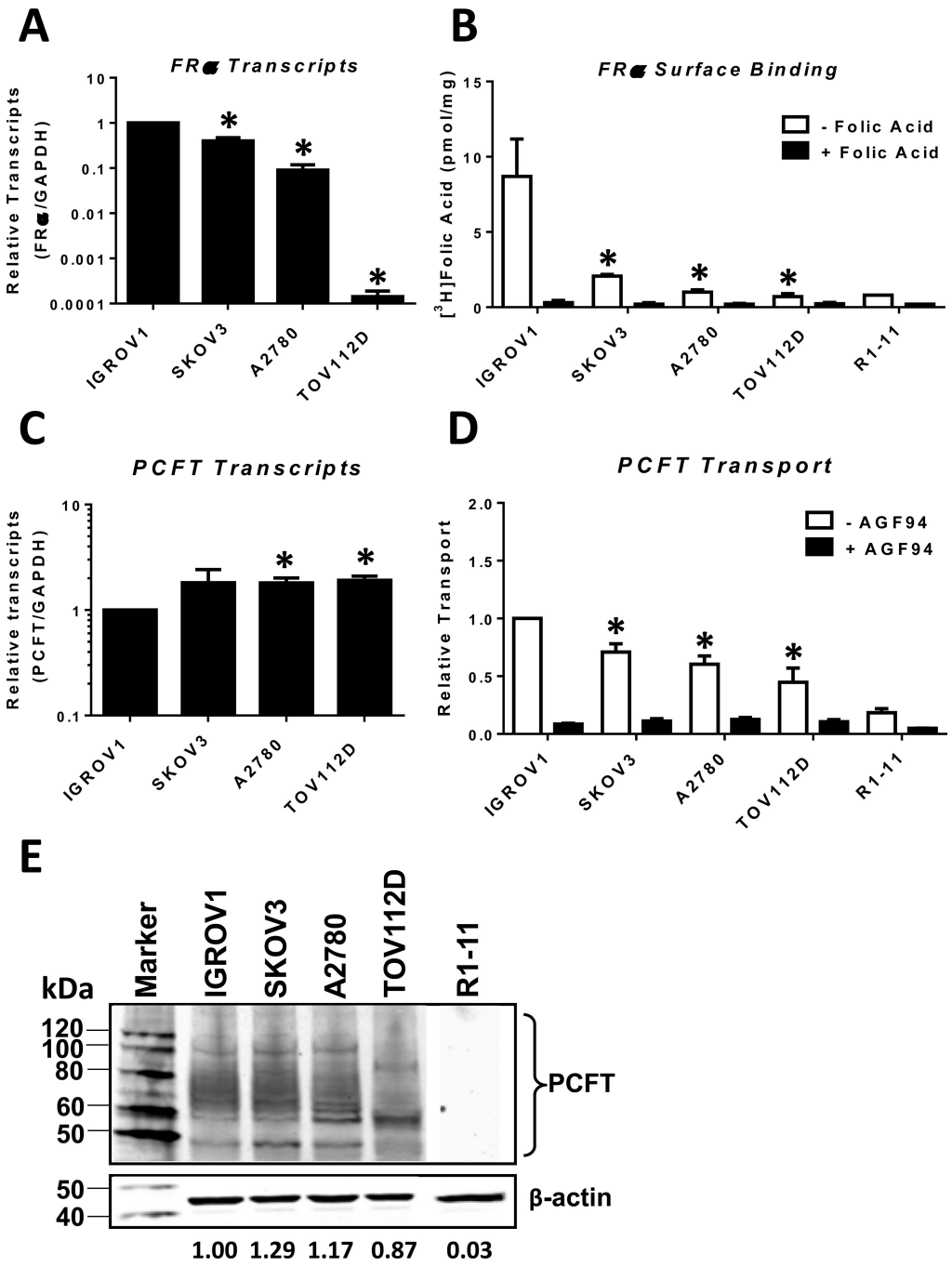

Figure 3. Characterization of FRα and PCFT in EOC cell line models, IGROV1, SKOV3, A2780, and TOV112D

Transcript levels for FRα (*Panel A*) and PCFT (*Panel C*) in IGROV1, SKOV3, A2780, and TOV112D EOC cell line models were measured by real-time RT-PCR and results are presented as mean values +/− standard errors from at least 3 experiments. FRα and PCFT transcript levels were normalized to transcript levels for GAPDH. FRα binding activities (*Panel B*) were determined with [^{3}H]folic acid at 0°C with and without unlabeled 10 μM folic acid; PCFT uptake (*Panel D*) was measured with [^{3}H]**AGF154** at pH 5.5 at 37°C for 5

min in the presence and absence of unlabeled 10 μM **AGF94**. Results are presented as mean values plus/minus standard errors from at least 3 experiments. Statistical significance between readouts for the assorted assays with the various EOC cell lines was analyzed by the unpaired t test. An asterisk indicates a statistically significant difference between the mean value for IGROV1 and the mean values for the other EOC cell lines ($p<0.0001$ for *Panel A*; $p<0.05$ for *Panel B*; $p<0.005$ for *Panel C*; and $p<0.05$ for *Panel D*). PCFT protein levels for the EOC cell line models were measured in crude plasma membranes by SDS-PAGE and Western blotting with PCFT polyclonal antibody (*Panel E*). A negative control (PCFT-null R1–11 HeLa cells) was run in the same gel as the other samples. This R1–11 lane was the same image in Figure 6D. β-Actin was used as a loading control. The molecular mass markers for SDS-PAGE are noted. Densitometry was performed using Odyssey software, and PCFT protein expression was normalized to β-actin. Representative densitometry results for the blot shown are noted. Variations in densitometry values between different blots (n=2) were within 10%.

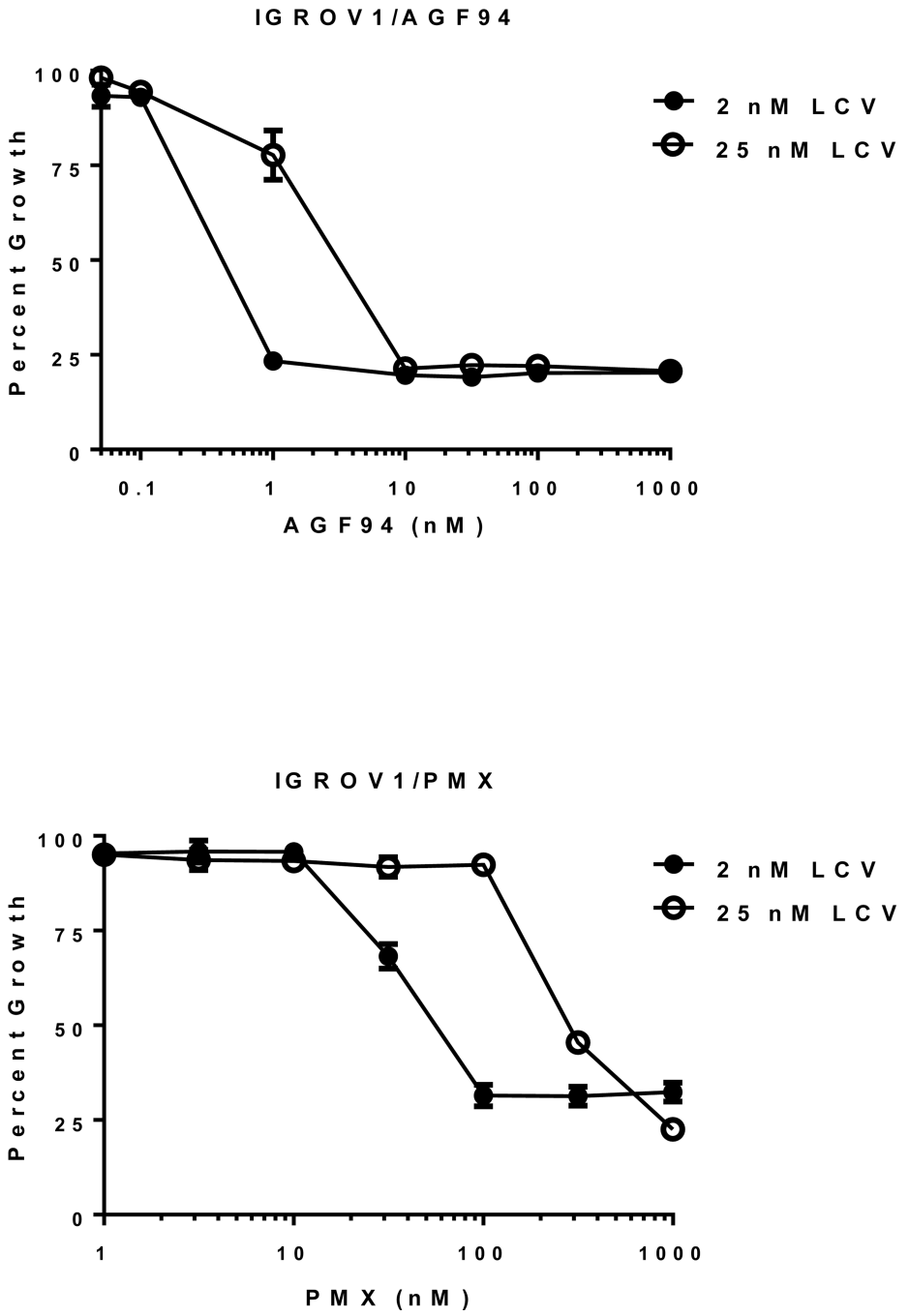

Figure 4. Drug sensitivities of IGROV1 cells to AGF94 and PMX at leucovorin (LCV) concentrations of 2 and 25 nM

Cells were plated (4000 cells/well) in folate-free RPMI 1640 medium with 10% dialyzed serum, antibiotics, L-glutamine, and 2 or 25 nM LCV with a range of concentrations of **AGF94** or PMX. Cell proliferation was assayed with CellTiter-Blue™ and a fluorescent plate reader. Results for drug treatments were normalized to relative growth in the absence of drug additions. Results are shown as mean values +/− standard errors (error bars) from 6 separate experiments. IC_{50}s for **AGF94** were 0.39 +/− 0.06 nM and 4.14 +/− 0.94 nM at 2

and 25 nM LCV, respectively. IC_{50}s for PMX were 57.7 +/− 3.0 nM and 346 +/− 26 nM at 2 and 25 nM LCV, respectively.

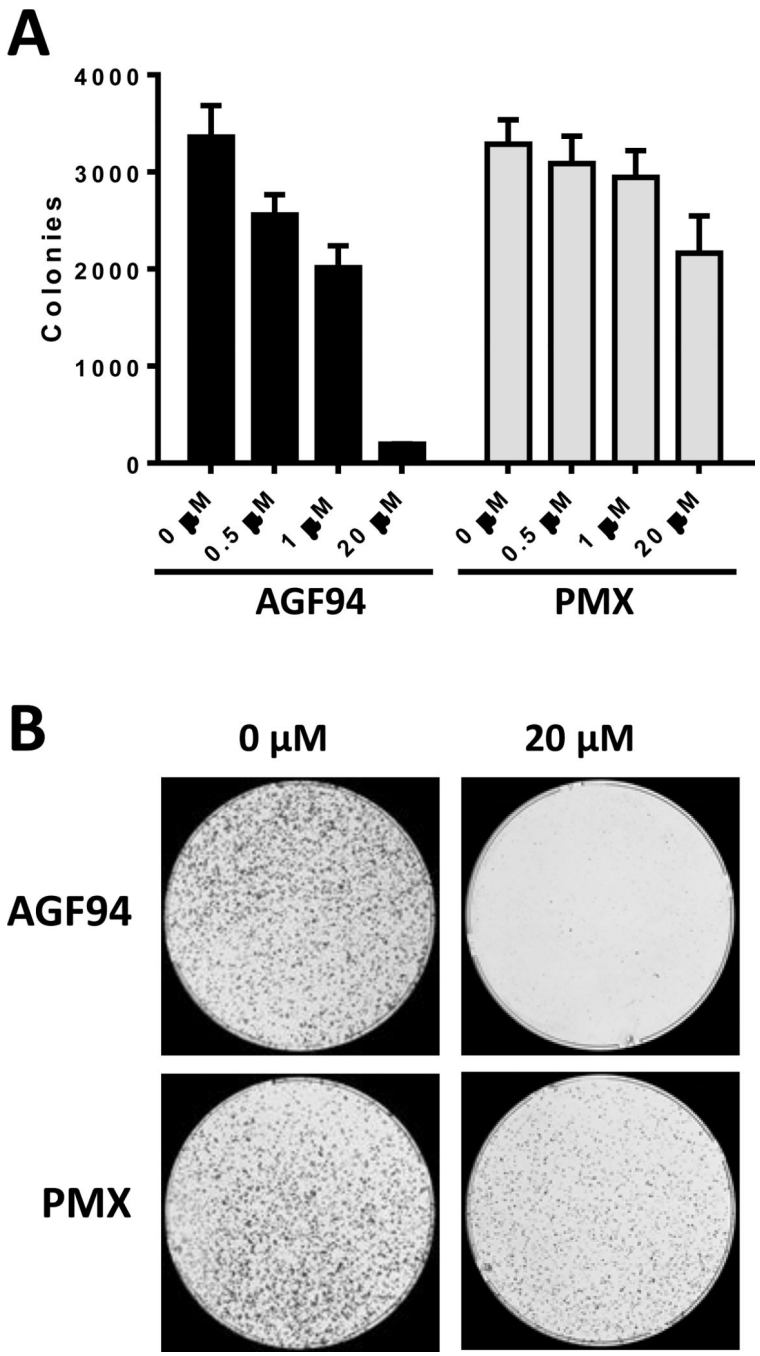

Figure 5. Cytotoxicity of AGF94 and PMX toward IGROV1 EOC cells

The cytotoxic effects of **AGF94** and PMX toward the IGROV1 EOC subline were assessed with colony-forming assays. IGROV1 cells (10,000 cells) were plated into 100 mm dishes in folate-free RPMI 1640 medium (pH 7.2), supplemented with 10% dialyzed fetal bovine serum, 1% penicillin/streptomycin, 2 mM L-glutamine, and 25 nM LCV. After 24 h, the cells were treated with **AGF94** or PMX (0, 0.1, 0.5, 1, 5, 20 μM) for an additional 24 h in the above media at pH 6.8. After drug treatment, the dishes were rinsed with Dulbecco's PBS, and complete folate-free RPMI 1640 medium (pH 7.2) with dialyzed fetal bovine

serum, antibiotics, and 25 nM LCV was added. Following incubation for 12 days, the dishes were washed with PBS, 5% TCA, and borate buffer (10 mM, pH 8.8). The colonies were stained with 1% methylene blue (in borate buffer), the dishes were rinsed (borate buffer), and colonies were counted with a GelCount™ colony counter (Oxford Optronix, UK). Results (n=3) are shown for the numbers of colonies counted relative to controls without drug (*Panel A*). Representative images of colony formation at 0 and 20 μM of **AGF94** or PMX are shown (*Panel B*).

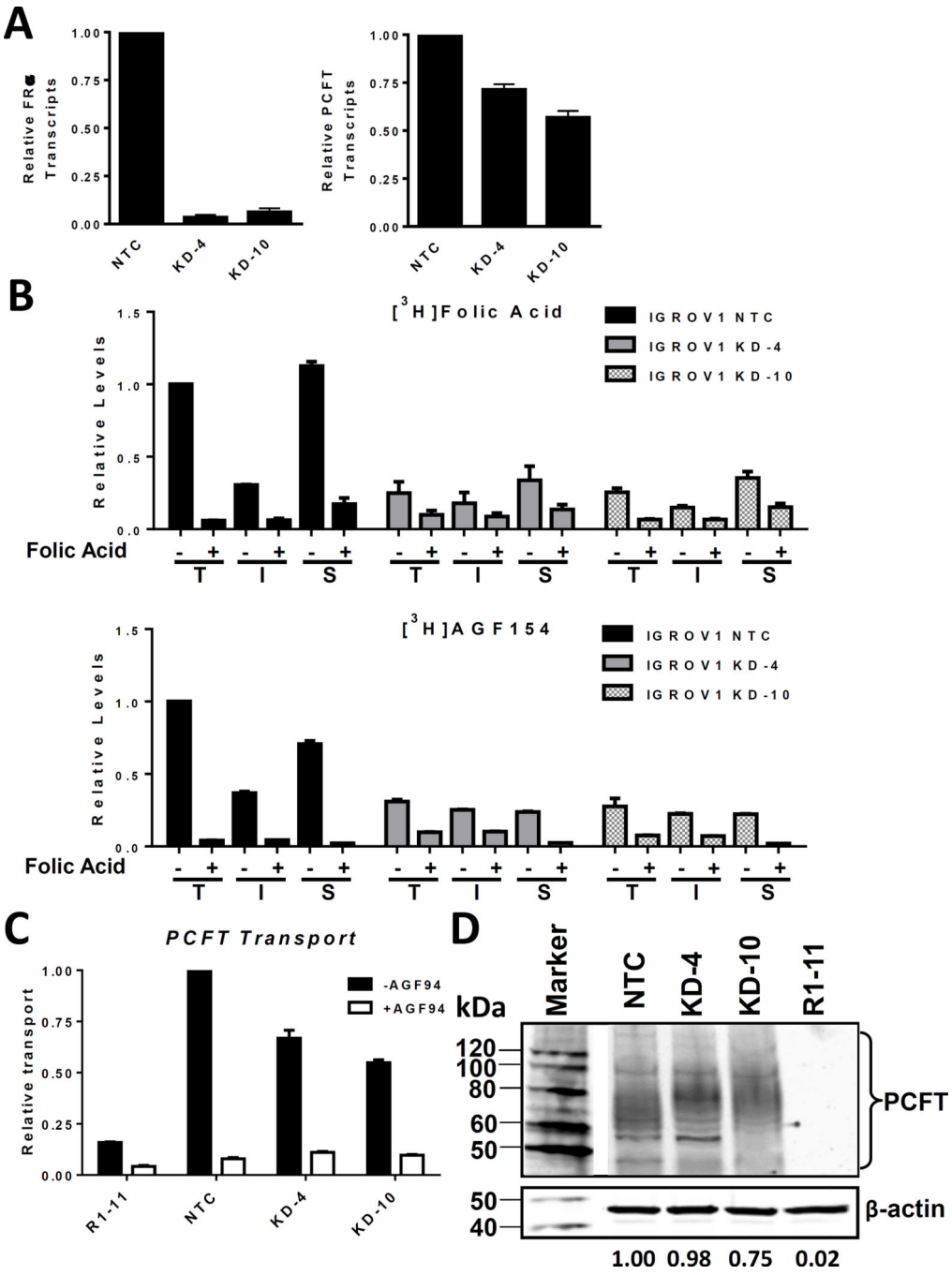

Figure 6. Effects of knockdown of FRα in IGROV1 cells on *in vitro* efficacy of 6-substituted pyrrolo[2,3 *d*]pyrimidine antifolates

FRα was knocked down in IGROV1 with lentivirus shRNA and clones (KD-4 and KD-10) were selected with puromycin. A scrambled shRNA was used as a non-targeted control (NTC). Results of 2~3 replicates are shown for FRα and PCFT transcript levels in IGROV1 NTC cells and KD-4 and KD-10 cells, measured by real time RT-PCR for FRα (*Panel A, left*) and for PCFT (*Panel A, right*). IGROV1 FRα KD clones were functionally characterized for FRα binding and uptake of [^{3}H]folic acid (upper *Panel B*) and

[^{3}H]**AGF154** (lower *Panel B*) at 37°C to measure total cellular (**T**) and intracellular (**I**) levels of [^{3}H]substrate, and at 0°C to measure surface (**S**) FRα-bound [^{3}H]substrate. These experiments were performed in the absence or presence of excess unlabeled folic acid (10 μM) as a competitor of FRα-mediated binding and uptake. IGROV1 FRα KD clones were also assayed for PCFT uptake (*Panel C*) with [^{3}H]**AGF154** at pH 5.5 at 37°C, in the absence and presence of 10 μM unlabeled **AGF94**. Results in *Panels B and C* are expressed as mean values +/− range (n=2). PCFT protein levels for the cell lines were measured in crude membranes by SDS-PAGE and Western blotting with PCFT antibody (*Panel D*). β-Actin was used as a loading control. The molecular mass markers for SDS-PAGE are noted. Densitometry was performed using Odyssey software, and PCFT protein expression was normalized to β-actin. Representative densitometry results for the blot shown are noted. Variations in densitometry values between different blots (n=2) were within 10%.

Table 1

Drug sensitivities of EOC cell line models, IGROV1, SKOV3, A2780, and TOV112D, and IGROV1 NTC, IGROV1 KD-4 and IGROV1 KD-10 sublines

Cells were plated (4000 cells/well) in folate-free RPMI 1640 medium with 10% dialyzed serum, antibiotics, L-glutamine, and 2 nM LCV with a range of concentrations of **AGF94, AGF154**, PMX, cisplatin, or PT523, in absence and presence of 200 nM folic acid (FA). Cell proliferation was assayed with CellTiter-Blue™ and a fluorescent plate reader. Results for drug treatments were normalized to relative growth in the absence of drug additions. Results are shown as mean IC_{50} values +/− standard errors (in parentheses) from 4 to 26 separate experiments. Abbreviation: ND, not determined.

Cell line	IC_{50}s									
	AGF94 (nM)		AGF154 (nM)		PMX (nM)		Cisplatin (μM)		PT523 (nM)	
	−FA	*+FA*	*−FA*	*+FA*	*−FA*	*+FA*	*−FA*	*+FA*	*−FA*	*+FA*
IGROV1	0.39 (0.06)	351 (48)	1.10 (0.24)	588 (64)	57.7 (3.0)	287 (10)	0.82 (0.09)	0.95 (0.11)	ND	ND
SKOV3	5.83 (2.14)	102 (18)	9.58 (1.89)	115 (20)	77.5 (5.5)	87.2(1.7)	5.03 (0.83)	5.76 (1.14)	ND	ND
A2780	0.44 (0.14)	29.5 (3.2)	2.65 (0.30)	71.7 (4.4)	19.4 (2.0)	39.7 (3.8)	1.07 (0.14)	1.37 (0.42)	ND	ND
TOV112D	81.1 (5.9)	182 (43)	110 (10)	419 (100)	48.9 (5.4)	57.1 (6.2)	7.02 (1.16)	8.64 (2.24)	ND	ND
IGROV1 NTC	0.72 (0.09)	197 (38)	1.47 (0.34)	372 (69)	88.8 (25)	157 (22)	ND	ND	3.39 (0.29)	3.70 (0.50)
IGROV1 KD-4	27.1 (7.5)	156 (46)	31.4 (11.5)	293 (51)	52.6 (7.7)	94.1 (13)	ND	ND	3.45 (0.42)	4.45 (0.58)
IGROV1 KD-10	12.2 (2.8)	203 (40)	28.5 (7.1)	477 (66)	100 (28)	127 (28)	ND	ND	3.23 (0.30)	3.22 (0.39)

Table 2

Antitumor efficacy evaluation of AGF94 against early stage human IGROV1 NTC and IGROV1 FRα KD-10 in female SCID mice

Eight week old female NCR SCID mice were implanted bilaterally subcutaneously with 30–60 mg tumor fragments by a 12-gauge trocar on day 0. Both tumor studies (IGROV1 NTC and IGROV1 FRα KD-10) used 4 mice per group. Chemotherapy was started on day 3 after tumor implantation, when the number of cells was small (10^7 – 10^8 cells). Median tumor masses were measured on day 31 for the IGROV1 NTC treatment arm and on day 24 for the IGROV1 FRα KD-10 treatment arm and were used to calculate T/C, T-C, and $\log_{10}$ tumor cell kill. Rx, treatment.

Tumor	Agent	Total dose (mg/kg)	Median tumor mass in mg (range)	T/C (%)	T-C (days)	Log_{10} kill
IGROV1 NTC	No Rx	–	622 (271 – 768)	–	–	–
	AGF94	128	180 (88 – 329)	29	15.5	1.0
IGROV1 FRα KD-10	No Rx	–	776 (523 – 938)	–	–	–
	AGF94	128	32.5 (0 – 297)	6	13	1.5